JOURNAL OF Applied Polymer SCIENCE

Characterization of Soda Hardwood Lignin and the Formation of Lignin Fibers by Melt Spinning

Abdul Awal, Mohini Sain
Centre for Biocomposites and Biomaterials Processing, University of Toronto, 33 Willcocks Street, Toronto, Ontario M5S 3B3, Canada
Correspondence to: A. Awal (E-mail: a.awal@utoronto.ca)

ABSTRACT: Lignin fibers were developed from a commercial available soda hardwood lignin (SHL) with a melt-spinning approach. SHL showed spinnability to form the fine fibers when poly(ethylene oxide) was used as a plasticizer with lignin. The thermal properties of lignin provided valuable information to assist the processing steps of the lignin fiber formation. The guaiacyl/syringyl ratio in SHL was determined by ^{31}P-NMR because it had great influence on the thermal mobility of lignin. A suitable temperature profile for the melt spinning was predicted through rheological studies of lignin. © 2013 Wiley Periodicals, Inc. J. Appl. Polym. Sci. 000: 000–000, 2013

KEYWORDS: biopolymers and renewable polymers; blends; fibers; rheology

Received 29 April 2012; accepted 28 November 2012; published online
DOI: 10.1002/app.38911

INTRODUCTION

Lignin is a renewable, commercially available, and low-cost biopolymer. It is an amorphous heteropolymer that confers the mechanical support of the plant.[1,2] According to Goring,[3] lignin is a random three-dimensional network polymer that is placed in the true middle lamella of wood and is composed of phenyl propane monomers linked together.

In addition, lignin is also a nonrandom two-dimensional network polymer that is found in the secondary wall.[4] After cellulose, lignin is the most abundant biopolymer on our planet, and it contains plenty of carbons.[5] Lignin is composed of three different types of phenyl propane units, as shown in Figure 1.

Lignins have dominant glycerol aryl ether (β-O-4) linkages, which act as a crosslinkers between short linear chains of phenyl propane units.[7] The monomeric units of lignin are connected by carbon–carbon and ether linkages through different connecting patterns; these lead to the complexity of the three-dimensional structure of lignin.[5,8] Different kinds of linkages in lignin and their diversity of functional groups result in a complicated macromolecule.[9] Lignin is generally obtained as byproduct from the pulp and paper industries. Most of the lignin is recovered from the pulping of black liquor, which is burned directly as fuel to recover the energy from the pulping process. The application of lignin can be significantly varied, depending on extraction technique and the types of sources. For example, there is a significant difference between hardwood kraft lignin and soda hardwood lignin (SHL) because of their chemical pulping processes. SHL is sulfur free, whereas hardwood kraft lignin contains sulfur from the pulping process. Lignin can be used as a dispersant, emulsifier, ion-exchange resin, water treatment agent, expander in the negative plates of lead acid surfactants, battery, pesticide sequestrating agent, binder, animal feed, and grinding aid and in electrolytic refining and tanning agents.[10–13] In addition, lignin could potentially be used to make carbon fibers that are suitable for the volume market with moderate the price levels. To reduce our dependency on petrochemical-based carbon fibers, enormous studies have been done on hardwood kraft lignin in the production of lignin fibers followed by carbon fibers.[12,14–16] Otani et al.[17] first developed lignin fibers to convert carbon fibers. After that, Sano et al.[18] produced lignin fibers from organosolv lignin. Next, Kubo et al.[19] tried to develop lignin fibers from softwood lignin. Recently, Kadla, Kubo, and coworkers[14–16] developed lignin fibers from hardwood kraft lignin and organosolv lignin. For better spinnability, they used poly(ethylene oxide) (PEO) as a plasticizer. The spinnability of lignin fibers increased significantly when PEO was used with lignin. According to their findings, hardwood kraft showed better spinnability compared to softwood kraft lignin. They assumed that softwood lignin had a highly condensed structure, which might have prevented the thermal mobility of the lignin during melt spinning.

According to literature studies, no attempts have been made to use sulfur-free SHL in the development of lignin fibers followed by carbon fibers. The yield of carbon fibers from SHL and hardwood kraft lignin is the same. However, SHL has no adverse

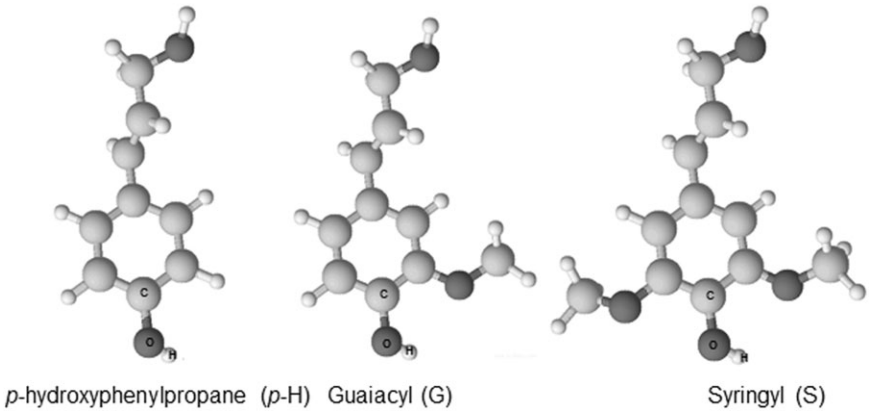

Figure 1. Three monomer building blocks of lignin.[6]

effect on the environment or human beings during thermal processing because it is sulfur free. Since no research has been conducted on SHL, it is important to study the thermorheological behavior of SHL and its different structures and melt-spinning capability.

The first objective of this study was to characterize SHL by differential scanning calorimetry (DSC), thermogravimetric analysis (TGA), and ^{31}P-NMR. In addition, rheological studies of SHL were conducted to predict the spinning parameters of the lignin fibers. The final aim of this study was to develop continuous lignin fibers from SHL with a melt-spinning approach. The obtained lignin fibers were characterized by scanning electron microscopy, and the spinnability of the fibers were examined.

EXPERIMENTAL

Materials

Hardwood lignin (eucalyptus) was supplied by GreenValue Co. (Punjab, India). The color of the lignin was yellow to light brown, and it had a strong straw odor. SHL was produced with a soda pulping process and contained no sulfur according to the supplier data sheet. The weight-average molecular weight of SHL was about 4000 g/mol.

PEO [viscosity average molecular weight (M_v) = 100,000] was purchased from Sigma-Aldrich (Oakville, Canada), and polypropylene (PP; PP 3622) was obtained from Arkema (Quebec, Canada). The melt flow index of PP was 12 g/10 min. Glycerol (density = 1.2 g/mL and water $\leq$ 0.5) was purchased from Sigma-Aldrich (Oakville, Canada). Poly(vinyl alcohol) (PVA; weight-average molecular weight = 13,000–23,000) was also purchased from Sigma-Aldrich (Oakville, Canada).

DSC and TGA

TGA was done with a TA Instruments Q500 (New Castle, USA) with a heating rate of 10°C/min. The samples were heated from 35 to 900°C to determine the complete thermal degradation of lignin. All tests were carried out in a nitrogen atmosphere with a flow rate of 60 mL/min. The softening temperature of hardwood lignin was determined with a TA Instruments Q1000 (New Castle, USA) differential scanning calorimeter equipped with a cooling system under a nitrogen atmosphere. The samples were run from 40 to 200°C with a heating rate of 10°C/min.

Sample Preparation for Quantitative ^{31}P-NMR Studies

A solvent mixture (25 mL) consisting of pyridine and deuterated chloroform (1.6 : 1.0 v/v) was made. The solvent mixture was protected from moisture by the addition of molecular sieves. A stock solution of the internal standard was prepared from 0.671 g of benzoic acid and 10 mL of the solvent mixture. Next, 1 mL of a stock solution of the internal standard was placed in a 10-mL volumetric flask containing 25 mg of dry relaxation agent [$Cr(acac)_3$]. Then, the volume was filled up to the 10-mL mark. Hardwood lignin (750 mg) was added to 25 mL of the solvent mixture with a small magnetic stirring bar. The mixture was stirred until the lignin was fully dissolved. Then, 2.5 mL of the phosphitylation agent (1,3,2-dioxaphospholanyl chloride) was added to it. The mixture was stirred and allowed to remain for 10 min to react. Finally, a 5-mL solution of internal standard (benzoic acid) and $Cr(acac)_3$ was added. The prepared sample was then placed in 5 mm $\times$ 203 mm tubes for ^{31}P-NMR acquisition and processing. All ^{31}P spectra were acquired on a Varian VNMRS spectrometer [$\nu(^1H)$ = 399.75 MHz, $\nu(^{31}P)$ = 161.82 MHz; Varian, Inc., Walnut Creek, CA] equipped with an AutoX probe. Spectra were acquired at 25°C over a 104–166.7 Hz spectral window with a 2-s recycle delay, 166–670 K complex points, and 200 transients. ^{31}P-NMR spectra were Fourier-transformed, phase-corrected, and baseline-corrected. Window functions, linear prediction, and zero filling were not applied before Fourier transformation. A 4-Hz line broadening was used for the processing of the spectra.

Rheological Properties of Lignin

The flow properties of lignin were investigated with a capillary rheometer (Rosand RH2000, Worcestershire, UK, radius = 15 mm and barrel length = 250 mm). Flowmaster software (Worcestershire, UK) was used to analyze the rheological data of lignin. Bagleys's correction was used to correct the entrance and exit pressure losses to provide the true wall shear stress (τ_w). The sample was placed in the barrel of the extrusion system and was pushed down into the capillary with a plunger. The residence time of lignin in the barrel was 10 min at temperatures of 180 and 200°C and 5 min at 210°C, and the melted lignin was extruded through the capillary at a preselected plunger speed. The experiments were conducted at different shear rates. The apparent shear rate ($\dot{\gamma}_a$) and τ_w were calculated from eqs. (1) and (2).[20,21] The equations were as follows:

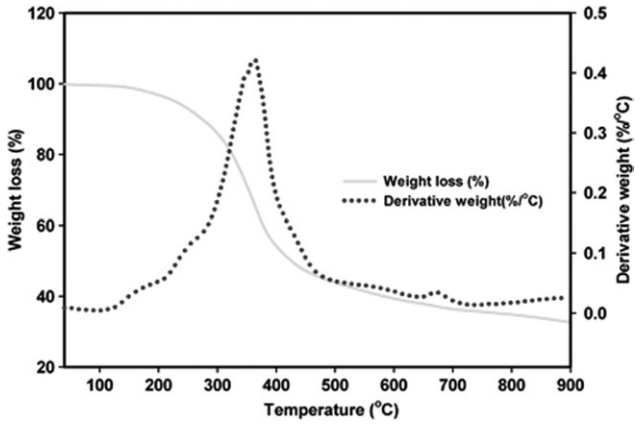

Figure 2. TG and differential thermogravimetry curve of SHL.

$$\dot{\gamma}_a = \frac{4Q}{\pi R^3} \quad (1)$$

$$\tau_w = \frac{\Delta P.R}{2L} \quad (2)$$

where Q is the volume flow rate (cm^3/s), R is the radius of the capillary, L is the capillary length, and ΔP is the pressure drop during extrusion. The power law index is the exponent in the expression, calculated by the following equation:[20,22]

$$\tau_w = K \cdot \dot{\gamma}_a^n \quad (3)$$

where k is the consistency index, n is the slope of the log τ_w against log $\dot{\gamma}_a$ plot. The flow behavior index was calculated as follows:[20,22]

$$n = \frac{d(\log \tau_w)}{d(\log \dot{\gamma}_a)} \quad (4)$$

A Rabinowitsch correction was used to calculate the true wall shear rate by the given equation:[17]

$$\dot{\gamma}_w = \left(\frac{3n+1}{4n}\right)\dot{\gamma}_a = \left(\frac{3n+1}{4n}\right)\frac{4Q}{\pi R^3} \quad (5)$$

The true shear viscosity (η) is termed as follows:[20]

$$\eta = \frac{\tau_w}{\dot{\gamma}_w} \quad (6)$$

Lignin Fiber Spinning

The lignin was dried at 160°C for 45 min to eliminate volatile substances. The lignin and synthetic polymer were mixed at various temperatures by a Brabender plasticorder mixer (Duisburg, Germany). The blended polymers were broken into small pieces by a hammer. Finally, the small-sized blended polymers were spun thermally with a rheometer (Rosand RH2000) equipped with a 1-mm spinneret. The spinning temperatures were selected depending on the type of polymer blends. The speed of the rheometer was controlled manually, and the residence time was 10 min.

RESULTS AND DISCUSSION

Thermal Properties of SHL

The thermal degradation of a polymer is a common phenomenon during thermal processing. The polymeric material starts degrading when it is processed at high temperatures. The processing conditions of a biopolymer or any synthetic polymer are set up below the decomposition temperature. Technically speaking, the temperature profile of the melt spinning of lignin is based on the data achieved from the thermogravimetric (TG) curve because the lignin shows both thermoplastic and thermosetting behavior. The spinning behavior of lignin is quite different from any other biopolymer or synthetic polymer because the lignin is a heterogeneous and complex mixture of copolymers. Virtually, the decomposition temperature of lignin will provide a maximum processing window for the process engineer to prevent thermal degradation. TG and differential thermogravimetry curve of SHL is shown in Figure 2. The first weight loss started at 122°C and could be associated with volatile substances, for example, water. The maximum decomposition temperature of lignin was about 366°C.

After we determined the degradation temperature of lignin, the glass-transition temperature (T_g) and the softening temperature of lignin were studied by DSC. T_g is the temperature at which the material changes its behavior from a glassy state to a rubbery state or from a rubbery state to a glassy state. DSC defines the glass transition as a change in the heat capacity as the polymer matrix goes from the glassy state to the rubbery state. The T_g of lignin is always influenced by the moisture content. To obtain a reliable T_g, the lignin sample was dried in an oven at 70°C for 24 h. The DSC result of SHL is shown in Figure 3. Normally, the T_g values of various nonderivatized lignins range from 90 to 180°C.

The T_g of hardwood lignin is about 126°C. An exothermic event was observed at 135°C for SHL lignin. The T_g of lignin provides a crucial message for the development of lignin fibers. Generally, when the extruded lignin exits from the spinneret or nozzle of the extruder, the thick fibers are drawn at high speed to get thinner fibers with molecular orientation before they reach the glassy state. As soon as the softened lignin moves from the rubbery to the glassy state, no further drawing is possible. The thermal behavior of lignin is changed if the lignin passed through the extruder several times. At some point, the lignin behaves like a thermoset polymer when the fiber formation is

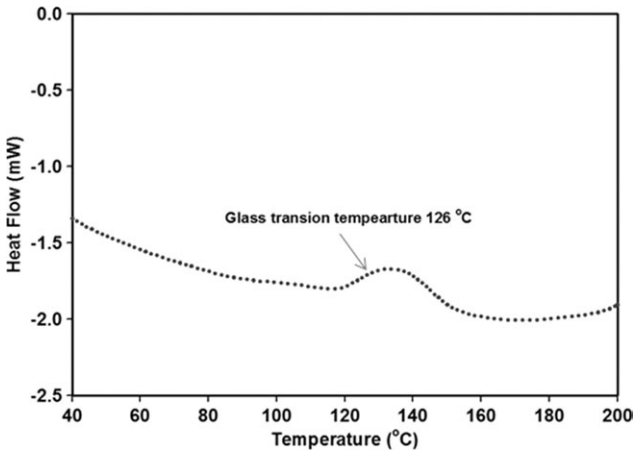

Figure 3. DSC curve for SHL.

Applied Polymer SCIENCE

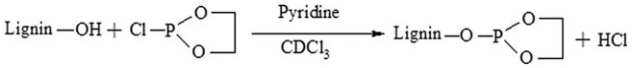

Figure 4. Phosphitylation reaction of labile protons in hardwood lignin with 1,3,2-dioxaphospholanyl chloride.

not possible. To overcome this unexpected problem during the melt spinning of lignin, the T_g of lignin works as an indicator.

Quantitative Analysis of Hardwood Lignin by ^{31}P-NMR

The ^{31}P-NMR spectra of hardwood lignin yielded two to three broad and two sharp resonances in the 140–125-ppm region corresponding to the phosphytilated hydroxyl groups within the lignin and the phosphytilated internal standard, benzoic acid. As discussed by Argyropoulos,[23] the broad peaks at 131.84 and 130.11 ppm were attributed to syringyl (S) hydroxyl groups and guaiacyl (G) hydroxyl groups, respectively. The small peak at 127.9 ppm corresponded to *p*-hydroxyphenyl hydroxyl groups. The peak for benzoic acid was observed at 127.5 ppm. The phosphitylation reaction with lignin is shown in Figure 4. The quantitative ^{31}P-NMR spectra of the hardwood lignin with the phosphitylating reagent 1,3,2-dioxaphospholanyl chloride are shown in Figure 5. The remaining peaks in the 140–125-ppm range did not account for the other hydroxyl, phenoxyl, or carboxyl groups within the lignin.

Table I shows the approximate chemical shift ranges for the different functional groups of lignin. The content and distribution of various hydroxyl groups in hardwood lignin are presented in Table II. It was important to know that the G, S, and *p*-hydroxyphenyl contents and their distribution in lignin because the ratio of G to S plays a vital role in the melt spinning of lignin. For example, a high content of G in softwood lignin is problematic in melt spinning because of its highly condensed structures. Since SHL has not been previously explored for melt spinning, the structural information for lignin was obtained to establish the relation between the chemical structure and properties of lignin fibers for future studies.

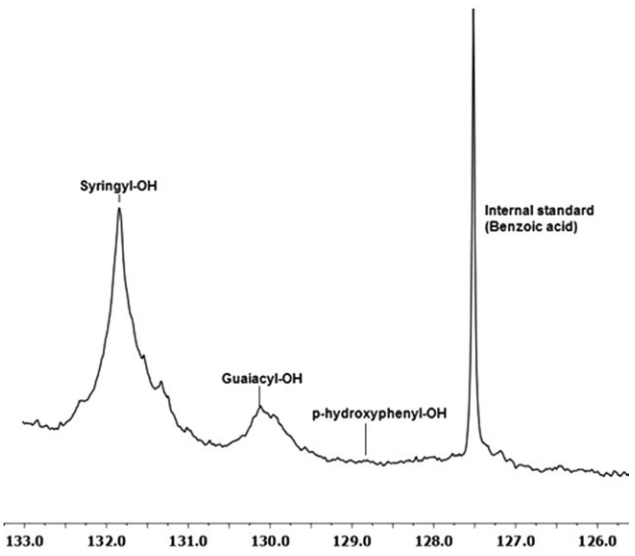

Figure 5. Quantitative ^{31}P-NMR spectra of hardwood lignin with phosphitylating reagent 1,3,2-dioxaphospholanyl chloride.

Table I. Chemical Shift Ranges in Different Functional Groups

Functional group	Chemical shift range integrated (ppm)
Internal standard (benzoic acid)	127.96-127.10
S—OH	132.22-131.57
G—OH	130.69-129.04
P-Hydroxyphenyl—OH	128.99-127.99

Table II. Content and Distribution of Various Hydroxyl Groups in Hardwood Lignin

Lignin sample	G—OH (mmol; %)		S—OH (mmol; %)		*p*-Hydroxy-phenl—OH (mmol; %)		Standard (mmol)
Hardwood	0.36	31.60	0.73	64.0	0.05	4.40	0.275

Rheological Properties of SHL

The rheology of the polymer is very crucial for optimizing the processing conditions and designing the different parts of the instrument, including the extruder, die, and melt-spinning equipment.[20] The flow properties of lignin offer important data regarding the viscosity, which is helpful in determining the optimum processing conditions during the melt spinning of lignin. In this study, the spinning temperature was predicted from flow curves. The flow behavior of hardwood lignin was investigated at different shear rates and temperatures of 180, 200, and 210°C. The temperatures were selected on the basis of the softening temperature of the lignin. The shear flow properties of lignin could be characterized by flow curves, where the shear viscosity is a function of shear rate. Generally speaking, the polymer solutions were non-Newtonian in character, and the rheological properties of the polymer depended on the shear rate and temperature.

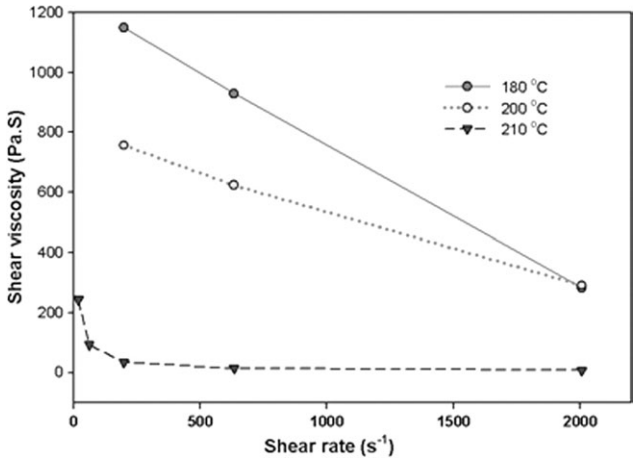

Figure 6. Relation between the shear viscosity and shear rate of hardwood lignin at different temperatures.

Table III. Processing Parameters of the Lignin-Based Fibers

Blending ratio	Mixing temperature (°C)	Spinning temperature (°C)	Spinnability
SHL	—	200	√
SHL/PEO			
95 : 5	180	190	√
90 : 10	180	190	√
80 : 20	170	190	√
SHL/PP			
80 : 20	210	210-220	Immiscible, thick strand
50 : 50	210	210-220	
SHL/glycerol			
97 : 3	180	180-190	—
95 : 5	180	180-190	—
SHL/PVA			
90 : 10	220	220-230	—
80 : 20	220	220-230	—

An em dash indicates that it was impossible to spin the fibers.

Table IV. Mechanical Properties of the Obtained Lignin Fibers with Compared to Literature Data

Lignin type	Tensile strength (MPa)	Modulus (GPa)	References
SHL	20 ± 1.40	2.89 ± 0.33	Our results
Hardwood kraft lignin	23	3.90	Kubo et al.[14]
Softwood kraft lignin	25	1.5	Uraki et al.[18]
Organosolv lignin	31	3.8	Kubo et al.[14]

The non-Newtonian character of the lignin polymer showed a great influence for the development of lignin fibers. As shown in Figure 6, the viscosity of hardwood lignin decreased with increasing shear rate; this demonstrated shear-thinning behavior, and similar viscosities were observed in the high-shear-rate region at temperatures of 180 and 200°C, respectively. In the low-shear-rate domain, the lignin demonstrated a considerable difference between the shear viscosities at various temperatures. As the shear rate increased, the viscosity of lignin became almost closer at a shear rate of 2000 s^{-1} because the viscosity of lignin decreased with increasing shear rate and temperature. However, the viscosity of lignin drastically decreased at a temperature of 210°C. The viscosity of hardwood lignin was found to be considerably different in the low-shear-rate region at temperatures of 180 and 200°C. Hardwood lignin exhibited both shear and temperature dependence viscosities. The shear rate and temperature significantly affected the shear viscosity with a non-Newtonian character. The viscosity of hardwood lignin could also be controlled through adjustment of the shear rate and temperature during extrusion or melt spinning.

The rheology of lignin was studied at three different temperatures to obtain the optimum spinning temperature. At a temperature of 180°C, the viscosity of the lignin was too high; this was considered the lower thermal mobility for spinning. On the other hand, the viscosity of the lignin at a temperature of 200°C was observed to be relatively low compared to that at a temperature of 180°C. At 210°C, the viscosity of the lignin was too low, and the lignin fibers could not form. From these rheological data, we selected a spinning temperature of 200°C, which was found to be an effective temperature for melt spinning. To validate the predicted temperature for spinning, the rheological studies and melt spinning were accomplished with the capillary rheometer using the same temperature profile. Our findings from the rheological data proved that the flow properties of the lignin were capable of predicting a suitable spinning temperature.

Spinnability of the Lignin Fibers

The spinnability of the lignin fibers were observed with and without the addition of plasticizer. The thermal mobility of the SHL lignin was good. However, the obtained lignin fibers from

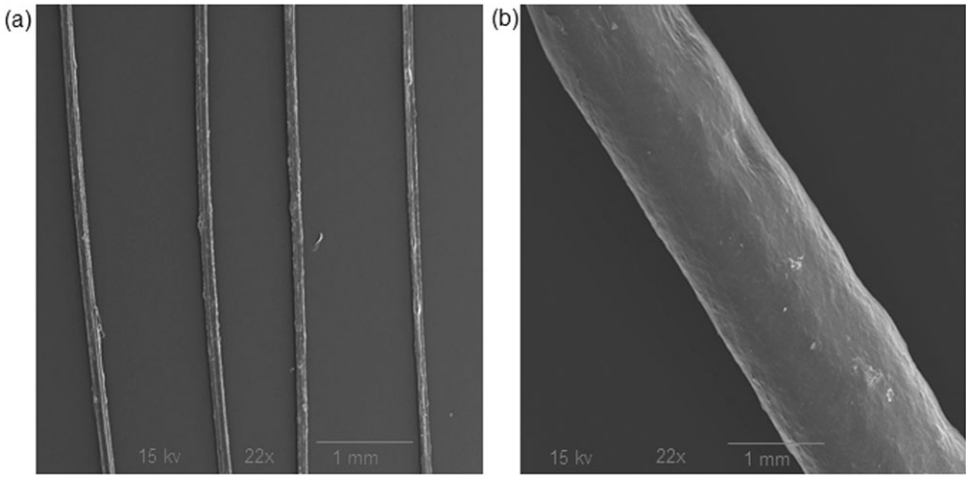

Figure 7. Scanning electron microscopy images of blended lignin fibers: (a) SHL/PEO (80/20) wt % and (b) SHL/PP (80/20) wt %.

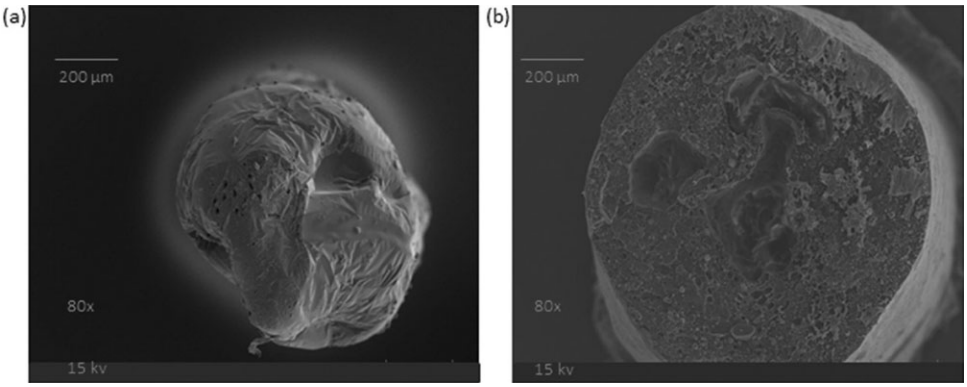

Figure 8. Cross section of the blended lignin fibers: (a) SHL/PEO (80/20) wt % and (b) SHL/PP (80/20) wt %.

SHL were brittle. To reduce the brittleness of the lignin fibers, different synthetic polymers were blended with lignin; the processing parameters are shown in Table III. To obtain sufficient spinnability, PEO was used with lignin as a plasticizer. The SHL/PEO blended fibers showed better spinnability and provided a higher flexibility compared to the neat-SHL-based lignin fibers. The spinnability of the blended fibers increased substantially with increasing content of PEO from 5 to 20 wt %. The blended fibers were spun continuously by a rheometer and were drawn manually. The developed fibers were cooled down to room temperature. The fiber surface of the SHL/PEO blends did not appear as smooth as the SHL/PP fibers (see Figure 7). The diameter of the fibers was found to be about 122 ± 17 μm because of the limitations of the drawing equipment. When the drawing speed was increased, the fiber diameter could be brought down to 15 μm because the addition of PEO with SHL increased the processability of the polymer blends. In addition, SHL and PEO were highly miscible in the blended fibers. The mechanical properties of the lignin fibers were compared with the literature data and are shown in Table IV. The tensile strength of the lignin fibers (SHL) were about 15 ± 2.34 MPa. Because of drawing, the tensile strength of the lignin fibers (20 ± 1.40 MPa) increased substantially. We believe that the molecular orientation occurred when the fibers were drawn during melt spinning; this resulted in better mechanical properties. The tensile strength of the blended fibers (SHL/PEO = 95 : 5) was about 11 ± 2.50 MPa; this was lower than that of the pure lignin fibers. The modulus of the lignin fibers (SHL) was about 2.89 ± 0.33 GPa, whereas the modulus of the blended fibers was about 2.5 ± 0.28 GPa. The strain percentage of the pure lignin fibers (0.53%) was significantly lower than that of the blended fibers (0.94%); this could have been an effect of PEO.

In contrast to the SHL/PEO blend fibers, the SHL/PP blended fibers showed poor spinnability because PP did not increase the processability of the mixed polymers during melt spinning. The fibers made from SHL/PP blends were thick, and the diameter of the fibers could not be reduced because the fibers were broken abruptly with increasing drawing speed (see Figure 7).

The SHL/PP blended fibers were not drawn at high speed because of their fragile behavior. The poor dispersion of PP in the composite system was confirmed through the observations of cross-sectional images of blended fibers (see Figure 8). The diameter of the fibers was about 1.04 ± 34 mm. Also, glycerol and PVA were used with lignin to generate the blended lignin fibers. In this case, no fiber spinnability was observed. The best fibers were developed from the combination of SHL and PEO polymers. These fibers could be investigated for the development of carbon fibers.

CONCLUSIONS

The thermal properties of lignin, such as the decomposition temperature, T_g, and softening temperature were very useful for starting the rheological experiments and melt spinning. The determination of the S/G ratio in lignin could be used to establish the structure–properties relation for future research. Rheological studies showed that the viscosity of SHL decreased with increasing shear rate; this demonstrated shear-thinning behavior with a non-Newtonian character. The rheological properties of SHL lignin predicted an appropriate temperature for melt spinning, which was successfully proven in the development of lignin fibers. Without loading plasticizer, the as-spun fibers from hardwood lignin were highly brittle. The hardwood lignin showed great spinnability with the addition of the plasticizer PEO up to 20 wt %. Lignin with PP showed poor spinnability as it was not miscible. These developed lignin fibers could potentially be used for the production of carbon fibers.

ACKNOWLEDGMENTS

The authors gratefully acknowledge the financial support of the Biofuel Waste Project provided by the Ontario Research Fund. The authors also thank to J. H. Lora for providing SHL for this study.

REFERENCES

1. Pérez, J. P.; Muñoz-Dorado, J. M.-D.; de la Rubia, T. D. L. R.; Martínez, J. M. *Int. Micro.* **2002**, *5*, 53.
2. Feldman, D.; Lacasse, M.; Beznaczuk, L. M. *Prog. Polym. Sci.* **1986**, *12*, 271.
3. Goring, D. A. I. In Lignin, Properties and Materials; American Chemical Society: Washington, DC, **1989**.

4. Glasser, W.; Sarkanen, S. Lignin Properties and Materials; American Chemical Society: Washington, DC, **1989**.
5. Sjöström, E. Wood Chemistry: Fundamentals and Application; Academic: Orlando, FL, **1993**.
6. Awal, A.; Sain, M. *J. Appl. Polym. Sci.* **2011**, *122*, 956.
7. Kubo, S.; Kadla, J. *Biomacromol.* **2005**, *6*, 2815.
8. Bocchini, P.; Galletti, G. C.; Seraglia, R.; Traldi, P.; Camarero, S.; Martinez, A. T. *Rapid Commun. Mass Spectrom.* **1996**, *10*, 1144.
9. Tejado, A.; Pena, C.; Labidi, J.; Echeverria, J.; Mondragon, I., *Biores. Tech.* **2007**, *98*, 1655.
10. Sarkanen, K. V.; Ludwig, C. H., Eds. Lignin: Occurrence, Formation, Structure and Reactions; Wiley-Interscience: New York, **1971**.
11. Hu, T. Q., Ed. Chemical Modification, Properties, and Usage of Lignin; Kluwer Academic/Plenum: New York, **2002**; p 10013.
12. Baker, F. S.; Gallego, N. C.; Naskar, A. K.; Baker, D. A. In FY 2007 Progress Report, ORNL; Oak Ridge National Laboratory: Oak Ridge, TN, **2007**.
13. Liu, Z.; Luo, X.; Li, Y.; Li, L.; Huang, Y. *Mater. Sci. Forum* **2009**, 620–622, 571.
14. Kubo, S.; Kadla, J. F. *J. Polym. Environ.* **2005** *13*, 97.
15. Kadla, J.; Kubo, S.; Venditti, R.; Gilbert, R.; Compere, A.; Griffith, W. *Carbon* **2002**, *40*, 2913.
16. Kadla, J. F.; Kubo, S. *Compos. A* **2004**, *35*, 395.
17. Otani, S.; Fukuoka, Y.; Igarasgi, B.; Sasaki, K. U.S. Pat. 3,461,082 (**1969**).
18. Uraki, Y.; Kubo, S.; Nigo, N.; Sano, Y.; Sasaya, T. *Holzforschung* **1995**, *49*, 343.
19. Kubo, S.; Uraki, Y.; Sano, Y. *Carbon* **1998**, *36*, 1119.
20. Ku, T.; Lin, C. *Text. Res. J.* **2005**, *75*, 681.
21. Abraham, T.; George, K. *Polym. Tech. Eng.* **2007**, *46*, 321.
22. Liang, J.-Z.; Li, R. K. Y. *J. Appl. Polym. Sci.* **1999**, *73*, 1451.
23. Argyropoulos, D. S. J. W. *Chem. Tech.* **1994**, *14*, 65.